C Journal of Carbon Research

MDPI

Review

Carbon Nanoarchitectonics for Energy and Related Applications

Rekha Goswami Shrestha [1], Lok Kumar Shrestha [1] and Katsuhiko Ariga [1,2,*]

[1] International Center for Materials Nanoarchitectonics (WPI-MANA), National Institute for Materials Science (NIMS), 1-1 Namiki, Tsukuba 305-0044, Japan; GOSWAMI.Rekha@nims.go.jp (R.G.S.); SHRESTHA.Lokkumar@nims.go.jp (L.K.S.)

[2] Department of Advanced Materials Science, Graduate School of Frontier Sciences, The University of Tokyo, 5-1-5 Kashiwanoha, Kashiwa 277-8561, Japan

* Correspondence: ARIGA.Katsuhiko@nims.go.jp

Abstract: Nanoarchitectonics has been recently proposed as a post-nanotechnology concept. It is the methodology to produce functional materials from nanoscale units. Carbon-based materials are actively used in nanoarchitectonics approaches. This review explains several recent examples of energy and related applications of carbon materials from the viewpoint of the nanoarchitectonics concept. Explanations and discussions are described according to the classification of carbon sources for nanostructured materials: (i) carbon nanoarchitectonics from molecules and supramolecular assemblies; (ii) carbon nanoarchitectonics from fullerenes; (iii) carbon nanoarchitectonics from biomass; and (iv) carbon nanoarchitectonics with composites and hybrids. Functional carbon materials can be nanoarchitected through various processes, including well-skilled organic synthesis with designed molecular sources; self-assembly of fullerenes under various conditions; practical, low-cost synthesis from biomass; and hybrid/composite formation with various carbon sources. These examples strikingly demonstrate the enormous potential of nanoarchitectonics approaches to produce functional carbon materials from various components such as small molecules, fullerene, other nanocarbons, and naturally abundant biomasses. While this review article only shows limited application aspects in energy-related usages such as supercapacitors, applications for more advanced cells and batteries, environmental monitoring and remediation, bio-medical usages, and advanced devices are also expected.

Keywords: biomass; carbon; composite; energy-related application; fullerene; hybrid; nanoarchitectonics; organic synthesis; self-assembly; supercapacitor

Citation: Shrestha, R.G.; Shrestha, L.K.; Ariga, K. Carbon Nanoarchitectonics for Energy and Related Applications. *C* **2021**, *7*, 73. https://doi.org/10.3390/c7040073

Academic Editor: Bruno C. Janegitz

Received: 17 September 2021
Accepted: 16 October 2021
Published: 19 October 2021

1. Introduction

Developments of functional materials are the foremost keys to solve various social problems such as energy [1–4], environmental [5–8], and medical issues [9–12]. As seen in materials fabrication processes based on organic synthesis [13–15], polymer chemistry [16–18], supramolecular chemistry [19–22], and materials sciences [23–26], carbon materials and hydrocarbon materials (organic compounds) play indispensable roles. Significant contributions of carbon-related materials originated in their high adaptability to various demands, their environmentally friendly nature, their possible biocompatibility, and the richness of their reserves in petroleum and biomass. Thus, one of the central players in materials science history is undoubtedly carbon.

In addition to producing materials with superior intrinsic properties, the importance of nanostructure controls of functional materials has been paid much attention in research efforts to produce more refined functional materials. This trend was triggered by nanotechnology developments, especially with advanced methods for observation and analyses on nanoscale structures [27–29]. Nanocarbons such as fullerenes, carbon nanotubes, and graphene derivatives play essential roles in various nanotechnology-related research efforts [30–32]. As seen in recent advanced observation techniques, nanocarbons such as

carbon nanotubes [33] and carbon nanohorns [34] were used for observation media. Furthermore, the accumulation of nanostructure analyses in functional materials has revealed the importance of nanostructure regulations for better performance.

As a one-step advanced methodology, nanoarchitectonics has been recently proposed as a post-nanotechnology concept (Figure 1) [35,36]. This concept was initially proposed by Masakazu Aono [37,38]. Nanoarchitectonics is a concept based on the fusion of nanotechnology with other research fields such as organic chemistry, supramolecular chemistry, fabrication processes, materials science, and bio-related science [39,40]. It is the methodology to produce functional materials from nanoscale units through combination/selection of atom/molecular manipulation, chemical conversion, self-assembly/self-organization, materials processing, and bio-related treatments [41,42]. Because the basic concept in nanoarchitectonics is universally applicable to a wide range of materials, the nanoarchitectonics concepts have been used for various targets including materials production [43,44], structure regulation [45–47], sensors [48,49], devices [50,51], catalysts [52,53], energy [54,55], environment [56,57], bioscience [58–60], and biomedical applications [61–63]. Carbon-based materials such as fullerenes are also used in nanoarchitectonics approaches [64,65].

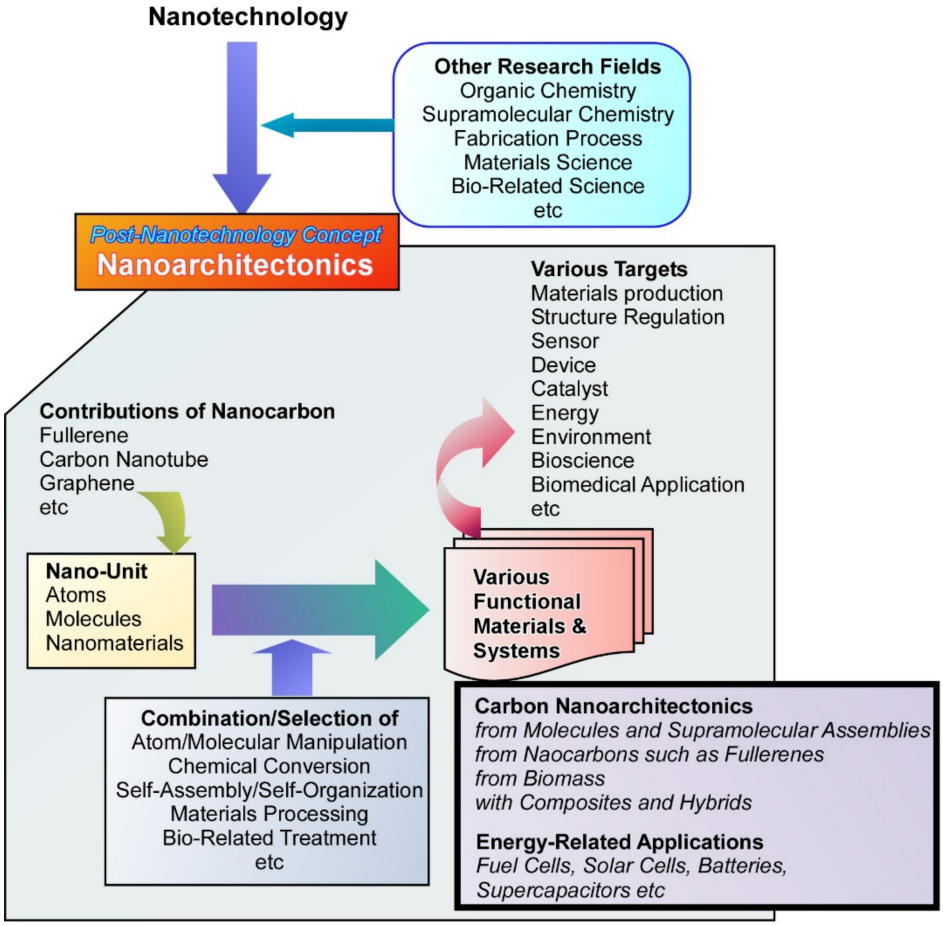

Figure 1. Outline of nanoarchitectonics concept to produce functional materials from nanoscale units with highlights of carbon nanoarchitectonics and its energy-related applications.

Although the term nanoarchitectonics has not appeared clearly, essences of the nanoarchitectonics approaches are used in the developments of various functional materials. Undoubtedly, carbon materials have significant contributions in recent research for functional materials. Nanocarbon materials, fullerenes, carbon nanotubes, and graphene are used for separation technology as stationary phases in both liquid and gas chromatography and solid-phase extraction [66]. Precise nanostructures such as the chirality of single-walled carbon nanotubes determine metallic or semiconducting natures, thus explaining devices'

usage of selectively extracted carbon nanotubes [67]. Not limited to precisely structured carbon materials, abundant carbon materials such as activated carbon materials are utilized for various applications. For example, it was reported that nitrogen-doped porous activated carbons were used for efficient separation between carbon dioxide gas and nitrogen gas based on promoted adsorption of carbon dioxide [68].

Among applications of nanostructured carbon materials, energy-related applications have been especially paid attention to. For example, nanoporous and mesoporous carbon materials have acquired elevated interest as the leading electrode materials for commercial supercapacitors [69,70]. Their characteristic features, especially their low production cost, outstanding cycle stability, wide voltage operating range, enhanced specific surface area, and porosity, make them the preference. These materials are widely explored as supercapacitor electrodes and sensing materials. As reported by Matsumoto and co-workers, graphene nanoribbons as narrow and elongated strips of graphene can be converted into interconnected pore materials [71]. Disordered structures in their uses for electrode materials are advantageous for capacitance retention, energy/power densities, and charge–discharge capability. Kawamura et al. investigated carbon electrode and solid-electrolyte interphase through operando measurement with in situ neutron reflectivity and ex-situ hard X-ray photoelectron spectroscopy during two-cycle battery operation [72]. Hysteresis behaviors of the amorphous carbon electrode upon lithiation/delithiation and chemical composition of the solid-electrolyte interphase layer were revealed. As summarized in the review by Matsuo, nanocarbon materials such as carbon nanotubes, fullerene derivatives, and endohedral fullerenes for stability improvements of organic and perovskite solar cells were investigated [73]. It was suggested that nanocarbon materials would have crucial roles in developing practical organic solar cells. As demonstrated in these examples, carbon materials have been used in various energy-related applications (Figure 1) where regulation and evaluation of nanostructures of carbon materials are crucial matters.

Based on these backgrounds, this review explains several recent examples of energy and related applications of carbon materials from the viewpoint of the nanoarchitectonics concept. Explanations and discussions are described according to the classification of carbon sources for nanostructured materials: (i) carbon nanoarchitectonics from molecules and supramolecular assemblies; (ii) carbon nanoarchitectonics from fullerenes; (iii) carbon nanoarchitectonics from biomass; and (iv) carbon nanoarchitectonics with composites and hybrids (Figure 1). Research examples described in this review article were not the best ones from the viewpoint of performances. These examples were selected for the demonstration of the wide applicability of carbon nanoarchitectonics.

2. Carbon Nanoarchitectonics from Molecules and Supramolecular Assemblies

Chemical conversion upon organic synthesis gives specific contributions in nanoarchitectonics processes at the molecular bottom level. For example, well-sophisticated organic synthesis can be used for syntheses of mimics of nanocarbon materials such as graphene derivatives and carbon nanotubes. As summarized in a recent review article by Xu, Müllen, and Narita, various large polycyclic aromatic hydrocarbon molecules can be organically synthesized as atomically precise graphene quantum dots [74]. Further extension of polycyclic aromatic hydrocarbon syntheses leads to the preparation of precisely structure-controlled graphene nanoribbons. These graphene quantum dots and graphene nanoribbons with precisely controlled strictures become nanocarbon materials with open bandgaps through the quantum confinement effect, unlike conventional zero-bandgap graphene. These nanoarchitected carbon molecules have high potentials in semiconductor-related applications such as nanoelectronics and optoelectronics. Upon the methodology of on-surface synthesis, scalable nanoarchitectonics for structure-defined graphene nanoribbon films can proceed on gold surfaces. In the recent research report, two nanographenes (dibenzohexacenohexacene and dibenzopentaphenoheptaphene) were prepared through on-surface synthesis using 8,8′-dibromo-5,5′-bibenzo[*rst*]pentaphene as a precursor (Figure 2) [75]. Precise structures of these prepared nanographenes were

confirmed by noncontact atomic force microscopy, and their electronic properties were estimated upon density functional theory calculations. Various applications such as quantum technologies, energy devices, optoelectronic devices, and bioimaging have been demonstrated for the organically synthesized nanocarbon materials.

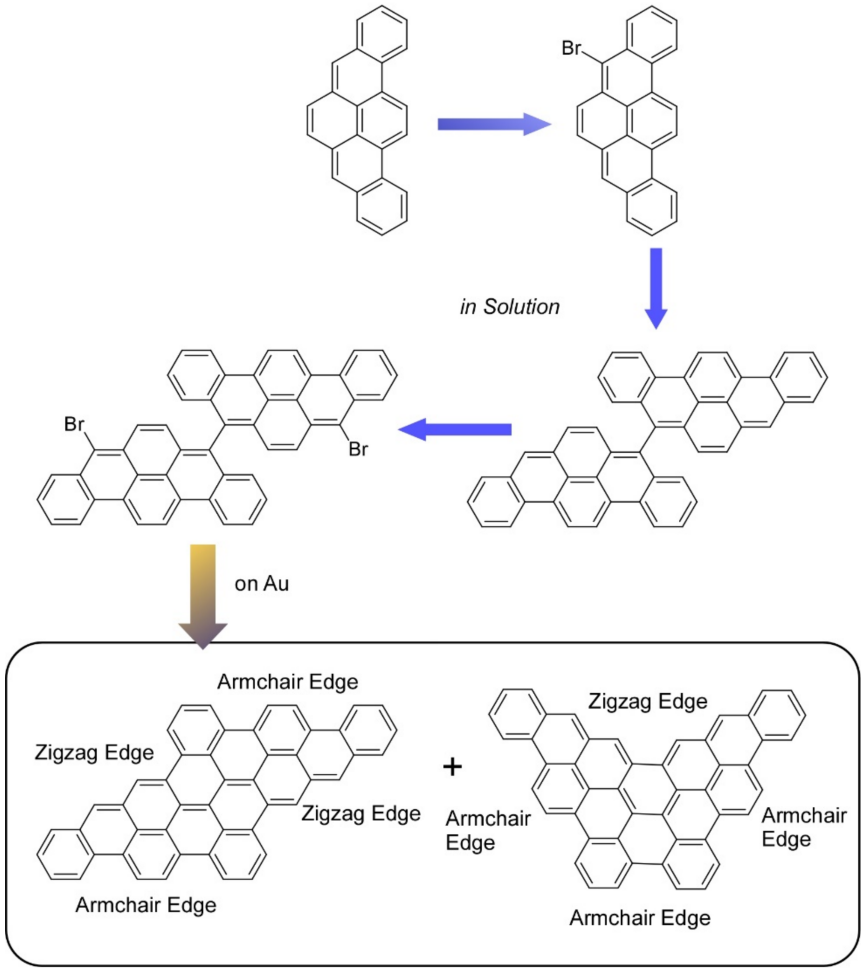

Figure 2. On-surface synthesis of two nanographenes (dibenzohexacenohexacene and dibenzopentaphenoheptaphene), using 8,8′-dibromo-5,5′-bibenzo[rst]pentaphene as a precursor.

Itami and co-workers recently reported the synthesis of supramolecular double-helix nanofibers upon self-assembly of negatively curved nanographene without any aids of assembly-assisting substituents (Figure 3) [76]. The used negatively curved nanographene molecules can work as gelators in various organic solvents to form double-helix structures through continuous $\pi-\pi$ stacking as confirmed by three-dimensional electron crystallography. The nanoarchitected one-dimensional supramolecular nanocarbon materials can be regarded as the first example of all-sp^2-carbon supramolecular π-organogelator with negative curvature. Isobe and co-workers designed and demonstrated the synthesis of finite phenine nanotubes with periodic vacancy defects [77]. The synthesized finite nanotube was a $C_{304}H_{264}$ molecule composed in a cylindrical shape having forty phenine units that are mutually connected at the 1, 3, and 5 positions. Its nanometer-sized cylindrical structure with periodic vacancy defects was identified crystallographically and spectroscopically. It was suggested computationally that fusion of these unit cylinder molecules resulted in carbon nanotubes, in which the periodic vacancy defects can modulate electronic properties of the synthesized nanotubes.

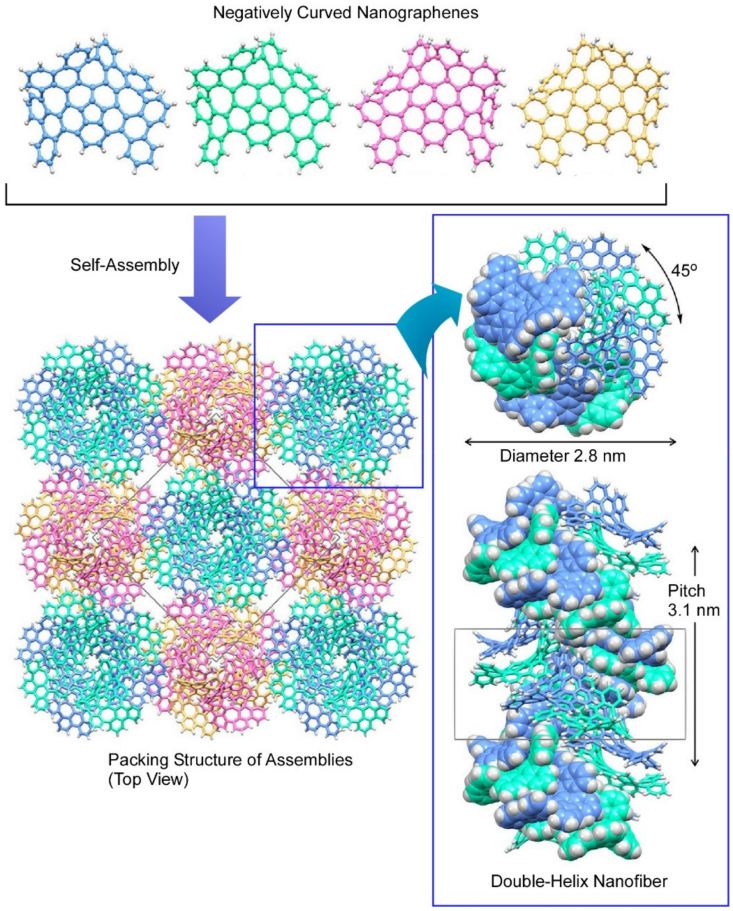

Figure 3. Formation of supramolecular double-helix nanofibers upon self-assembly of negatively curved nanographene. Reprinted with permission from Reference [76]. Copyright 2021 American Chemical Society.

Nanocarbon films were fabricated by self-assembly of ring-shaped organic molecules with mechanical motions at a two-dimensional liquid interface [78]. Carbon nanoring molecule, 9,9′,10,10′-tetra-butoxy-cyclo[6]-paraphenylene-[2]-3,6-phenanthrenylene, dissolved in chloroform was on the water subphase with gentle rotational vortex motion. This vortex Langmuir–Blodgett (vortex-LB) method [79–81] made the carbon nanoring molecules uniformly assemble into a molecular thin film at the air–water interface. The assembled thin film was transferred onto a solid substrate, followed by carbonization of the transfer film for transformation to carbon nanosheet at elevated temperatures under nitrogen gas flow. The finally obtained nanofilm had a two-dimensional uniform morphology with a thickness of about 10 nm. If nitrogen-containing molecules such as pyridine were mixed into the carbon nanoring precursor, nitrogen-doped carbon nanosheets were synthesized. The electrical conductivity of the nitrogen-doped carbon sheets was significantly enhanced. The nanoarchitected carbon nanosheets would have potential in uses as catalysts for oxygen-reduction reactions for high-performance fuel cells. This conventional synthetic method is also advantageous for the large-scale production of nanocarbon materials. Haino and co-workers very recently demonstrated the production of nanographene materials from carbon sources through acid-assisted oxidative carbon cleavage with post-treatments of neutralization and deionization [82]. Size separation using dialysis membranes provided nanographene with a specific size distribution.

Template synthesis using molecular assemblies and other nanomaterials as sacrificial templates is a powerful method to produce various nanostructured materials such as mesoporous silica [83–85]. This strategy is also applied to carbon nanoarchitectonics, as seen in the preparation of nanoporous and mesoporous carbon materials [86,87]. Wide ranges of

applications have been investigated for such porous nanocarbon materials. As summarized in the recent review article by Vinu and co-workers, nanoporous carbon materials with a sufficiently high surface area have high potential in environmental applications such as removing toxic heavy metals and radionuclides from water [88]. For adsorption efficiency and selectivity, surface functional properties and textual characteristics are crucial factors. These features can be adjusted by processes through selection and combination of the precursors, synthetic conditions, activation, and modification. Especially, the low-cost nature of preparation processes for nanoporous carbon materials is advantageous for a worldwide application for water remediation. Shitanda et al. demonstrated the use of pendant glycidyl group-modified mesoporous carbon materials as stable supports of enzymes [89]. Flavin-adenine-dinucleotide-dependent glucose dehydrogenase immobilized on mesoporous carbon materials exhibited a glucose-oxidation catalytic current using 1,2-naphthoquinone as the redox mediator. Such enzyme-coupled nanostructured carbon materials can be applied as bioelectrodes for biofuel cells. Vinu and co-workers demonstrated the preparation of two-dimensional mesoporous C_{60}/carbon hybrid materials for usages in supercapacitor and Li-ion battery applications (Figure 4) [90]. The nanotemplating method using mesoporous silica SBA-15 as a template was used for the synthesis of mesoporous fullerene/carbon hybrids, which were subjected to usages as electrodes for Li-ion battery and supercapacitance applications. It was revealed that carbon coatings on the mesoporous fullerene were important factors in energy storage devices.

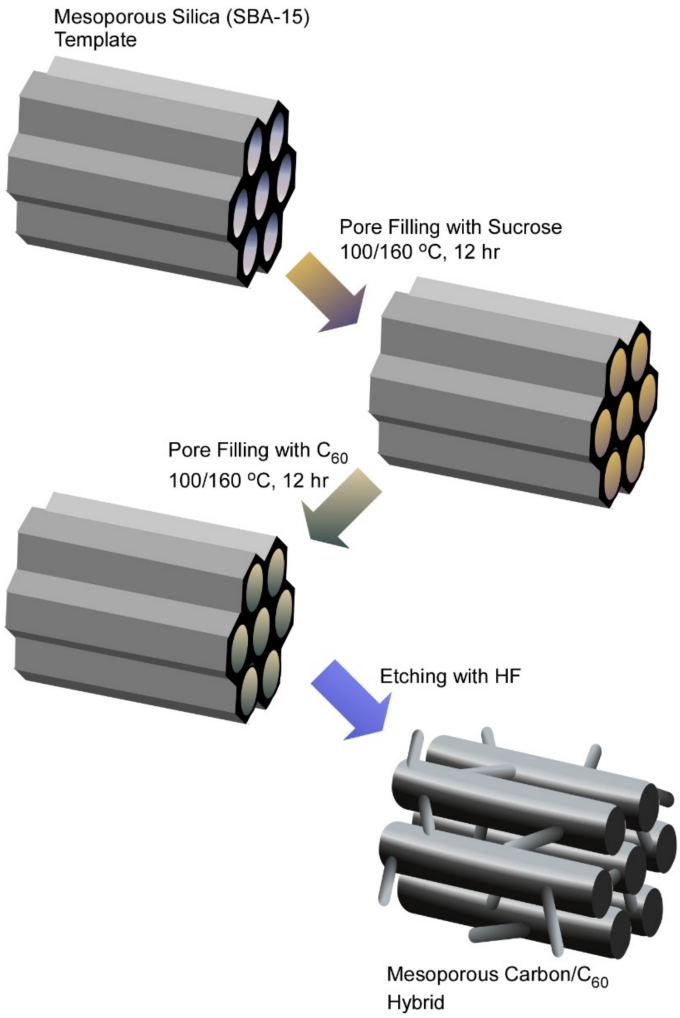

Figure 4. Preparation of mesoporous C_{60}/carbon hybrid materials through nanotemplating method using mesoporous silica SBA-15 as a template.

As popularly researched, nanoporous materials, metal-organic frameworks, and coordination polymers have been widely researched [91–93]. These coordination-based materials can be converted to porous carbon materials that have been researched for energy-related applications. Henzie, Yamauchi, Na, and co-workers reported nanoarchitectonics of the fabrication of flexible micro-supercapacitors using nanocarbon films derived from the zeolitic imidazole-based metal-organic framework (ZIF-8) (Figure 5) [94]. Flexible micro-supercapacitors were fabricated through rather a conventional electrophoresis technique. The porous carbon films fabricated on micro-supercapacitors exhibited superior electrochemical performance. The easily processable nature of this electrophoresis method for high-quality, uniform nanoarchitected carbon films with good electrical conductivity would become a powerful method for the preparation of excellent electrochemical devices. It would have important contributions to miniaturized and flexible power supplies in future applications. Covalent-organic frameworks have also been paid much attention as another type of functional porous material [95–97]. The conversion of covalent organic frameworks to nanoporous carbon materials has also investigated. Kim, Shiraki, and Fujigaya recently reported the preparation of nitrogen-doped nanoporous carbon materials through thermal conversion of triazine-based covalent organic frameworks [98]. The fabricated nanoporous carbon materials basically have large surface areas with bimodal microporous and mesoporous structures. Their pore textures can be modified by modification of carbonization temperatures. Condition optimization for the synthesis of the nitrogen-doped porous carbons would result in good capacitive performance.

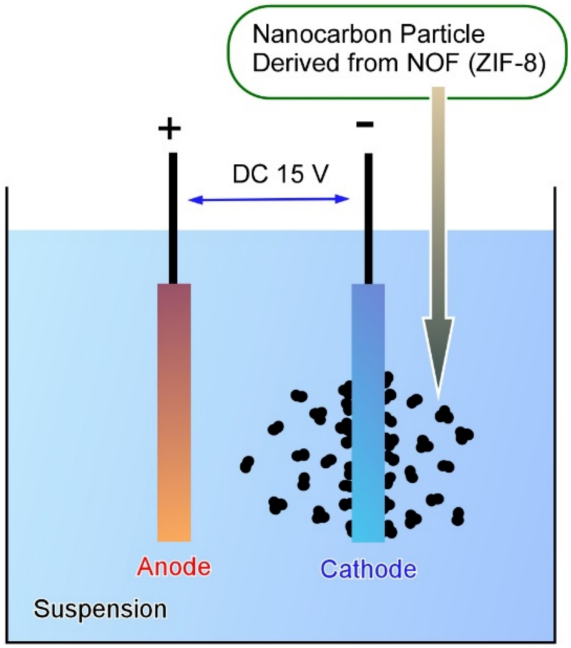

Figure 5. Fabrication of the flexible micro-supercapacitor electrodes using nanocarbon films derived from the zeolitic imidazole-based metal-organic framework (ZIF-8).

3. Carbon Nanoarchitectonics from Fullerenes

Fullerene is regarded as a zero-dimensional molecule. It can, however, self-assemble into higher one-dimensional, two-dimensional, and three-dimensional morphologies [99,100]. The self-assembled nanostructures of fullerene molecules have high symmetries and extended conjugated π-systems that impart unique physical and chemical properties. The functional performance of any device depends mainly on its nanoarchitectonic morphology. Therefore, there is a tremendous effort to innovate new methodologies to design various self-assembled nanostructures to tailor their functional properties strategically. Several potential applications of fullerene-based nanomaterials have been explored in biomedicine, semiconductors, optics, electronics, and spintronics [101,102]. Furthermore,

introducing well-defined mesoporous architectures with controllable pore sizes of these fullerene nanostructures can increase their surface areas and synergistic interactions and provide multiple functionalities, which is usually impossible to achieve using conventional materials. Thus, fullerene with such architectures can be employed in several applications, including high-performance solar cells, supercapacitors, hydrogen storage, photocatalysts, and sensing [103,104]. However, constructing complex hierarchical functional materials over different length scales using functional molecules, particularly fullerene C_{60} or C_{70} remains challenging.

Fullerene (C_{60}) is a stable spherical allotrope of carbon. It has 20 hexagonal and 12 pentagonal rings, with a network of sixty structurally equivalent sp^2-hybridized carbon atoms. It can form various self-organized structures involving π-stacking and strong van der Waals interactions. Energetically unfavorable double bonds in its rings make it a perfect candidate to design novel devices in diverse fields, including optoelectronics, photovoltaics, sensing, etc. The formation of highly graphitic walls with extended conjugated π-systems in nanoporous carbons would enhance its electrical conductivity and improve its durability; strategic design of the self-assembled structures is still an area to explore. In this context, a novel method for large-scale and ultra-rapid fabrication of fullerene nanorods and nanotubes has been recently demonstrated. Additionally, nanoporous fullerene nanorods and nanotubes as ideal π-electron carbon sources having π-electron conjugation within the sp^2-carbon with robust frameworks for electrochemical capacitor and sensor applications are also demonstrated.

For example, one-dimensional fullerene (C_{60}) nanorods and fullerene nanotubes were fabricated using the liquid–liquid interface precipitation method [105]. Fullerene nanotubes were obtained at an interface formed between a saturated solution of C_{60} in mesitylene and isopropyl alcohol. In contrast, fullerene nanorods were produced at an interface between a saturated solution of C_{60} in mesitylene and *tert*-Butyl alcohol through careful mixing at 25 °C. The low polydispersity was observed for both fullerene nanorods and fullerene nanotubes. Both fullerene nanorods and fullerene nanotubes were composed of individual C_{60} single crystals. One-dimensional single-crystal fullerene nanorods and fullerene nanotubes were then converted to nanoporous carbon nanorods and nanoporous carbon nanotubes, respectively, by heating directly at a very high temperature (up to 2000 °C) in a vacuum (Figure 6). This yields a new family of nanoporous carbons with sp^2-carbon robust frameworks with graphitic walls having π-electron conjugation within. The original one-dimensionality of the fullerene nanorods and fullerene nanotubes was retained. Following this strategic experimental design, a drastic increase in the effective surface area (nanoporous carbon nanorods = 1600 $m^2\ g^{-1}$ and nanoporous carbon nanotubes = 1650 $m^2\ g^{-1}$) could be achieved. These nanoporous carbon nanorods and nanoporous carbon nanotubes showed enhanced electrochemical capacitance (specific capacitance of 145.5 $F\ g^{-1}$ (for nanoporous carbon nanotubes) and 132.3 $F\ g^{-1}$ (for nanoporous carbon nanorods) at a scan rate of 5 $mV\ s^{-1}$). Quartz crystal microbalance experiments with nanoporous carbon nanotubes showed outstanding sensitivity and selectivity towards solvent molecules, especially aromatic molecules. The sp^2-bonded graphitic carbon frameworks in nanoporous carbon nanotubes make the π–π interaction between them and solvent molecules possible, allowing easy and free diffusion of aromatic solvent molecules into the nanopores.

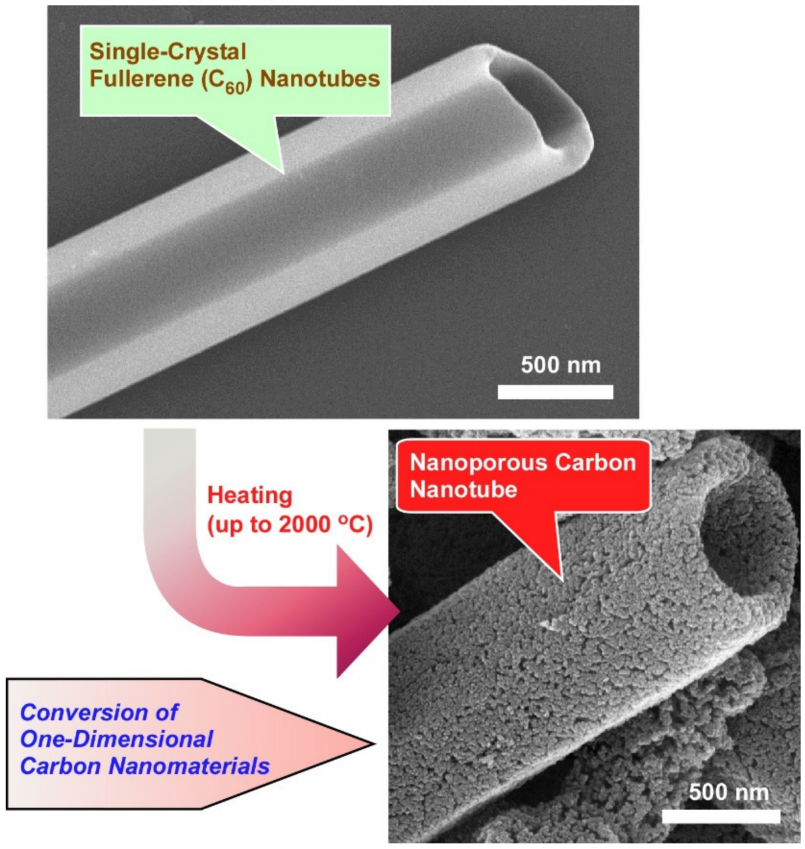

Figure 6. Conversion of one-dimensional single-crystal fullerene (C_{60}) nanotubes to nanoporous carbon nanotubes by heating directly at very high temperature (up to 2000 °C) in vacuum.

Fabrications of mesoporous crystalline fullerene (C_{70}) microtubes with highly crystalline pore walls and their direct conversion into mesoporous graphitic carbon microtubes were also reported (Figure 7) [106]. First, mesoporous fullerene C_{70} tubes were synthesized using an ultrasonic liquid–liquid interfacial precipitation method. Briefly, fullerene C_{70} tubes were fabricated at the interface formed between the solution of fullerene (C_{70}) in 1,2-dichlorobenzene and isopropyl alcohol, at 15 °C, followed by sonication and multiple washing to remove 1,2-dichlorobenzene completely. The fullerene C_{70} tubes were then used as a π-electron carbon source to produce high surface area mesoporous graphitic carbon with crystalline pore walls. Furthermore, direct conversion of fullerene C_{70} tubes was directly converted into mesoporous graphitic carbon microtubes by heat treatment at 2000 °C in a vacuum, with the initial one-dimensional tubular morphology retention. The walls of the resulting graphitic carbon microtubes are composed of ordered conjugated sp^2 carbon with a robust mesoporous framework structure. The electrochemical supercapacitance performance of mesoporous graphitic carbon microtubes was studied (mesoporous graphitic carbon microtubes modified glassy carbon electrode in 1 M H_2SO_4) through cyclic voltammetry and chronopotentiometry (charge–discharge) measurements. It was found that this new carbon material exhibits high specific capacitance ca. 212.2 F g^{-1} at a scan rate of 5 mV s^{-1} and 184.6 F g^{-1} at a current density of 0.5 A g^{-1}. It is believed that an innovative methodology towards the fabrication of a new type of nanoporous carbon material with graphitized frameworks would open up a new avenue for the fabrication of multifunctional carbon nanomaterials, which are not attainable by traditional approaches to prepare mesoporous/nanoporous carbons, for high-end applications such as solar cells, supercapacitors, hydrogen storage materials, and sensors.

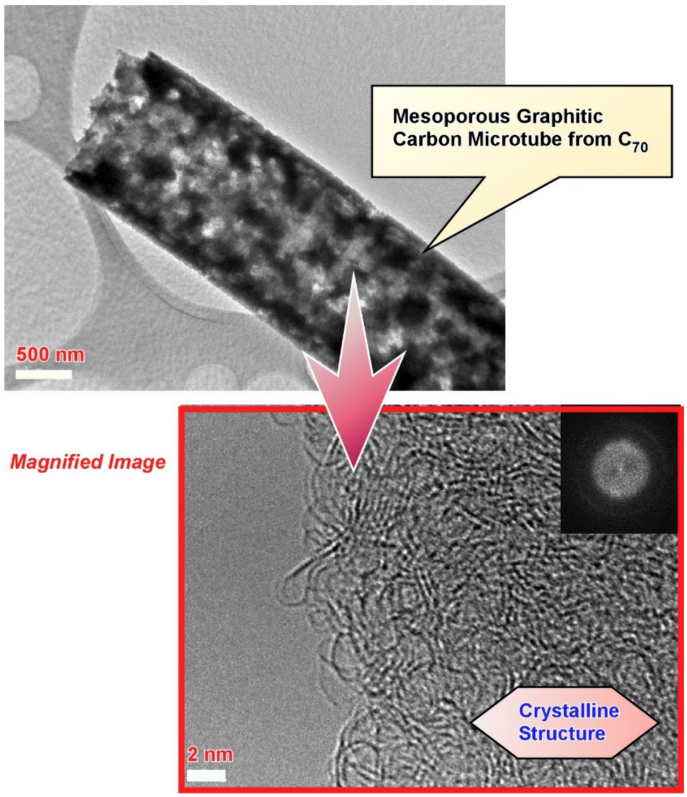

Figure 7. Mesoporous graphitic carbon microtubes fabricated from mesoporous crystalline fullerene (C_{70}) microtube.

4. Carbon Nanoarchitectonics from Biomass

In addition to exclusive nanocarbon materials such as carbon nanotube, graphene, reduced graphene oxide, and fullerene, nanoporous carbon materials can also be derived from natural biomass like lignite, coal, peat, wood, etc. [107,108]. There are several methods for obtaining nanoporous carbons from natural biomass like direct carbonization, the chemical activation method, template methods, etc. Of all the popular methods, physical and chemical activation methods represent the feasible, scalable, and low-cost methods. Physical activation involves heating precursor material at high temperatures in the air, nitrogen, carbon dioxide, or steam. Low yield and product with a low surface area are the demerits of this method. While in chemical activation, the precursor material is treated with dehydrating salts such as zinc chloride ($ZnCl_2$), potassium chloride (KCl); acids like phosphoric acid (H_3PO_4) and sulfuric acid (H_2SO_4); and alkalis like sodium hydroxide (NaOH) or potassium hydroxide (KOH). The activation is done before carbonization at relatively low temperatures. This decomposes lignocellulosic materials pyrolytically. Nanoporous carbons with enhanced porosity are obtained with less energy input through these methods. The porosity can be controlled by controlling the activation temperature, time, and impregnation ratio of the activating agents. Specific surface area and pore volumes of chemically activated nanoporous carbons are much higher than physically activated carbons. Additionally, their fabrication process is also cost-effective and straightforward. Therefore, they are preferably explored as electrode materials for electrical double-layer capacitors. Extensive research has been procured in the production of such nanoporous carbon materials using various sources of agricultural wastes or biomass as precursor materials such as rice husks, pistachio shell, pitch, coconut shell, bamboo, corncob, corn husks, firewood, oil-palm shell, etc.

Biomass-derived nanoporous activated carbons exhibit very high surface areas and porosity because of their unique ordered micro- and meso-porous architectures. In addition, they show good electrical conductivity and admirable electrochemical stability, which are

highly desired in the emerging electrochemical energy storage supercapacitors applications. Bamboo is a naturally abundant lignocellulosic material that contains cellulose, hemicellulose, and lignin as the chief components. Through carbonization, decomposition of these chief polymeric structures is expected, leaving behind a rigid carbon skeleton. Fabrication of nanoporous carbon from bamboo cane powder through chemical activation with phosphoric at comparatively very low activation temperature, 400 °C, was reported [109]. They have thoroughly investigated their surface area, pore volume, electrochemical supercapacitance, and sensing performance and the effect of the impregnation ratio of phosphoric acid on them. The nanoporous carbon formed was amorphous with well-ordered miro- and mesopores. It was found that both the surface area and the pore volume could be controlled by controlling the impregnation ratio of phosphoric acid and that of bamboo cane powder. The surface area was found in the range from 218 to 1431 $m^2\ g^{-1}$ and pore volume in the range from 0.26 to 1.26 $cm^3\ g^{-1}$. The nanoporous carbon exhibited electrical double-layer capacitor behavior with a specific capacitance of 256 F g^{-1} at a scan rate of 5 mV s^{-1}. In 1000 cycles of cyclic stability test (charge and discharge), a 92.6% capacitance retention was observed.

Adsorption of toxic solvent vapors on nanoporous carbons has received considerable attention. Several reports support the fact that well-designed porous materials with high surface area and large pore volume show a high affinity towards vapor sensing [110,111]. Nanoporous carbon obtained from bamboo cane powder exhibited brilliant surface and structural properties. Furthermore, vapor sensing properties of nanoporous carbon towards volatile organic solvents were also studied using the quartz crystal microbalance technique (Figure 8). The nanoporous carbon lacks a well-developed graphitic microstructure that could assist the adsorption of aromatic solvent vapors (π–π interactions between solvent molecules and the sp^2-bonded graphitic carbon framework). Therefore, they exhibited higher sensitivity for non-aromatic solvent vapors like methanol and ethanol than aromatic vapors like benzene and toluene. At the same time, sensitivity towards non-aromatic solvent vapors could be due to the presence of oxygen-containing surface functional groups (–OH, C=O, and COOH) in nanoporous carbon, which promotes interactions between oxygen and alcohol vapors to their adsorption. Further, this material showed discrimination between ethanol and methanol. Because methanol has a higher density of the interactive site (OH per one carbon) than ethanol (OH per two carbons), methanol naturally interacts more towards these functional groups than the latter. Therefore, nanoporous carbon prepared from naturally abundant bamboo could apply in separation and selective sensing of these volatile chemicals widely expected in the petroleum and food industries.

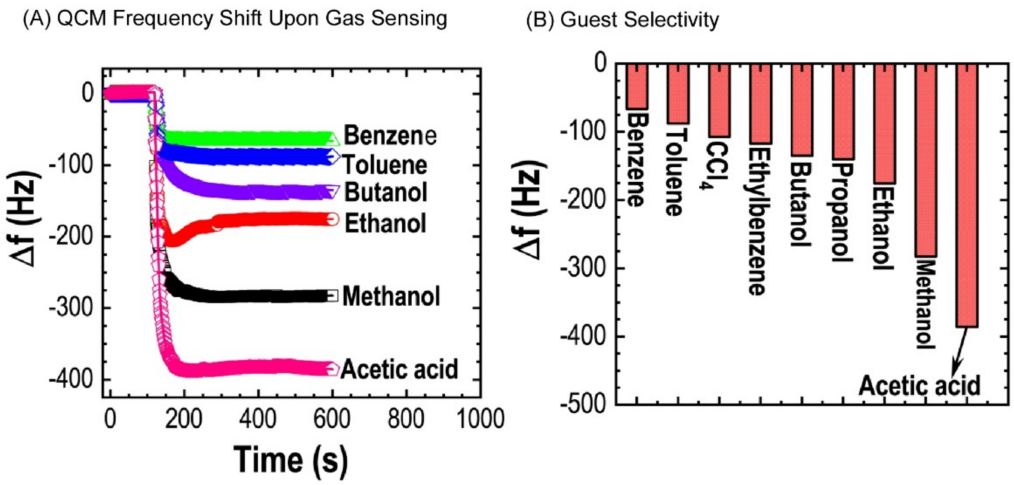

Figure 8. (**A**) QCM frequency shifts quartz crystal microbalance coated with nanoporous carbon upon exposure to methanol, ethanol, butanol, benzene, toluene, ethylbenzene, and acetic acid; (**B**) summary of sensing performance [109].

Xu, Wang, Hossain, and co-workers fabricated porous carbon materials from lignocellulose for the capacitive deionization applications [112]. The porous nanocarbons were synthesized through direct carbonization of lignocellulose. The obtained porous carbon materials have several advantages for capacitive deionization applications, including a high production yield, cost-effectiveness, and environmentally friendly natures. These characteristics are desirable ones for industrial-level capacitive deionization applications. Nitrogenated porous carbon materials often have promoted performances in capacitive deionization. Xu, Zhang, and Yang reported the synthesis of nitrogen-doped porous carbon microtubes by pyrolyzing naturally abundant biomass (willow catkins) with the nitrogen source of urea [113]. Highly enhanced desalination performance was observed for porous carbon microtubes with high nitrogen content compared with undoped analogues. Liu, Zhang, and co-workers fabricated O-N-S co-doped carbon from the Lotus leaf stem with multiscale pore architecture [114]. The proposed preparation methods based on pre-carbonization and KOH activation can be scalable. The fabricated O-N-S co-doping carbon materials possess three-dimensional hierarchical structures with high surface area and desirable distribution of pore sizes. Advantageous features for supercapacitors, including a large accessible surface for charge storage, low internal resistance, rapid charge transfer, and short ion diffusion distance, can be expected.

Generally, desirable requirements in biomass precursors for the preparation of activated carbon include high abundance, cost-effectiveness, high carbon content, and ease of activation. Lapsi (choerospondias axillaris) seed stone satisfies all of the above properties. It is abundantly available in its native country Nepal, and the seed is an agricultural waste product, with a high carbon content; additionally, it can be easily carbonized to obtain activated carbon. Therefore, Lapsi seed could be suitable for the fabrication of nanoporous activated carbon materials that could be low-cost electrode material for high-performance electrochemical supercapacitors and even candidates for sensing volatile organic compounds. The preparation of nanoporous carbon materials with a high surface area was actually prepared from Lapsi seed through $ZnCl_2$ activation, one of the preferable activating agents over sulfuric acid, phosphoric acid, potassium hydroxide, or potassium carbonate, etc. at a moderate temperature, 700 °C [115]. It was confirmed that the nanoporous carbon has an amorphous structure incorporating oxygen-containing functional groups. It was also found that the nanoporous system contained graphitic carbon structures with interconnected hierarchical micro- and mesopores (Figure 9). Surface areas and pore volumes of the materials were found, in the ranges from 931 to 2272 $m^2\ g^{-1}$ and 0.998 to 2.845 $cm^3\ g^{-1}$, respectively, which were better than commercial activated carbons. Its potential as electrode material for supercapacitors was explored because of its high surface areas, large pore volumes, and interconnected hierarchical micro- and mesoporous structures. The glassy carbon coated with this nanoporous carbon in 1-M H_2SO_4 aqueous solution showed brilliant electrochemical supercapacitance. The maximum specific capacitance of 284 F g^{-1} at a current density of 1 A g^{-1} was observed. The electrodes exhibited a high-rate capability with 67.7% capacity retention at a high-current density of 20 A g^{-1}. High capacitance retention (99%) with excellent cycle stability in 10,000 charge–discharge cycles was achieved, demonstrating the potential of Lapsi seed-derived nanoporous carbons as suitable electrode materials in high-performance supercapacitor devices. The results demonstrated that nanoporous activated carbon derived from Lapsi seed, a form of agricultural waste, could be suitable as electrode materials for high-performance supercapacitor devices.

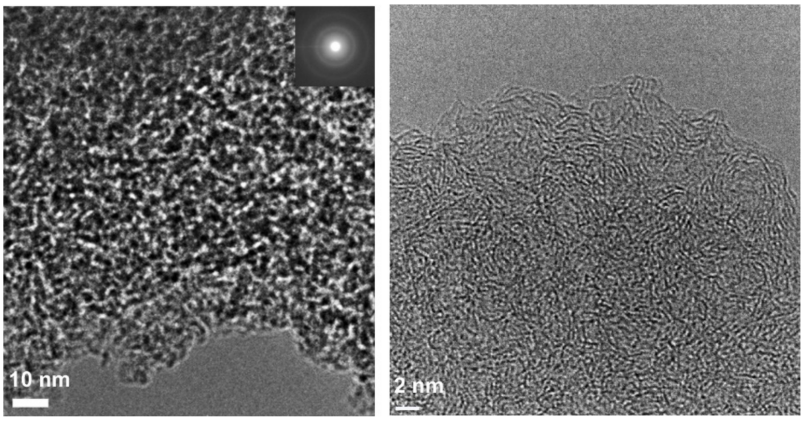

Figure 9. Nanoporous carbon fabricated from Lapsi seeds containing graphitic carbon structures with interconnected hierarchical micro- and mesopores.

Nanoporous activated carbon materials were fabricated from the natural agro-waste precursor, washnut seed, using $ZnCl_2$ as a dehydrating chemical (activating agent) [116]. The activation temperature range was 400–1000 °C. The nanoporous carbon obtained through $ZnCl_2$ activation of washnut at different temperatures exhibited an ordered micro- and mesoporous structure. The surface area and the porosity of the nanoporous carbon greatly depended on the carbonization temperature. The higher the temperature, the higher was the surface area and the porosity. The highest specific surface area (1309 $m^2\ g^{-1}$) and pore volume (0.789 $cm^3\ g^{-1}$) were observed at 800 °C. The electrochemical performance of the thus obtained nanoporous carbon-modified glassy carbon electrode was studied in an aqueous solution of 1 M H_2SO_4 on three-electrode cells. Nanoporous activated carbon obtained at 800 °C showed the best surface textural properties like higher surface areas, well-defined porosity, and an ordered micro- and meso-porous structure with graphitic walls. Therefore, this sample also showed excellent electrochemical supercapacitance, with a specific capacitance of 225.1 F g^{-1} at a current density of 1 A g^{-1}. A capacitance retention of 69.6% at a high current density of 20 Ag^{-1} indicated a high-rate capability of the nanoporous carbon as an electrode material. A 98% cycling stability was observed in the test of 10,000 charging–discharging cycles. These results demonstrate that washnut seed, an agro-waste precursor, could be utilized to produce nanoporous carbon with enhanced surface textural properties. This material can be used as a low-cost and scalable supercapacitor electrode for high-performance supercapacitors.

5. Carbon Nanoarchitectonics with Composites and Hybrids

Instead of synthesizing nanostructures of one particular material, nanoarchitectonics of composites and/or hybrids sometimes become rational ways to achieve advanced functions [117,118]. For example, Jakmunee and coworkers reported the fabrication of nanocomposites with carbon nanotubes, nickel oxide, and Nafion for electrocatalytic detection of serotonin and dopamine in human serum [119]. Facile electroanalytical detection of serotonin with rapid, selective, and sensitive features is highly desired. Therefore, electrocatalytic sensing systems based on screen-printed carbon electrodes modified with carbon nanotubes/nickel oxide/carbon black/Nafion were tested especially for serotonin detection among other interfering species. The nanoarchitected sensing systems exhibited several advantageous features for serotonin detection, including a low limit detection, a wide linear range, and high reproducibility, as well as a good recovery range.

Materials exhibiting enhanced capacitances and a long cycle lifetime have received significant attention. It is possible to obtain such materials by combining electrical double-layer capacitors and pseudocapacitors called hybrid supercapacitors. Therefore, a comprehensive exploration of such hybrid supercapacitors is understandable. For the electrode materials of electrical double-layer capacitors, carbon-based nanomaterials such as fullerene, carbon nanotube, reduced graphene oxide, and mesoporous or nanoporous

carbons have been widely explored, while for the electrode materials for pseudocapacitors, several transition metal oxides have been broadly explored. Carbon nanotubes and reduced graphene oxides have higher carrier mobility and electrical conductivity. Therefore, they are preferably used as the matrix of a hybrid supercapacitor. Furthermore, there are several nanocomposites that are widely explored as electrode materials in supercapacitor applications, such as binary nanocomposites of carbon nanotubes, graphene-based materials, conducting polymer polyaniline, or polyaniline composite with metal sulfide or oxide with metal oxide nanoparticles [120,121]. Nanostructures and properties of materials greatly influence the performance of supercapacitors. Therefore, it is understandable that the hierarchical micro-/nano-structures must be explored to enhance device performance.

Following the footsteps in the formation of a novel material for the advanced supercapacitors, fabrication of ternary nanocomposite material composed of mesoporous nanocube indium oxide (In_2O_3) of size 50 nm embedded into carbon nanotubes and reduced graphene oxide was reported (Figure 10) [122]. The ternary nanocomposite, In_2O_3/carbon nanotubes/reduced graphene oxide, was fabricated through the hydrothermal method. Microscopic images showed that mesoporous nanocrystals of In_2O_3 were uniformly dispersed on the π-electron-rich conductive nanocarbons, the carbon nanotube, and the reduced graphene oxide nanocarbon surface. The electrochemical supercapacitance performance of nanocomposite was tested by modifying a glassy carbon electrode nanocomposite material. It showed an enhanced/appreciable specific capacitance of 1273 F g^{-1} at 5 mV s^{-1} and 948 F g^{-1} at 1 A g^{-1}. In addition, they exhibited outstanding cyclic stability. The capacity loss of the nanocomposite-modified electrode was not observed even after 5000 charge/discharge cycles. Additionally, capacitance retention was calculated as 75% at a high scan rate of 200 mV s^{-1}. These outcomes from the cyclic voltammetry and chronopotentiometry measurements establish the fact that this integrated In_2O_3/carbon nanotube/reduced graphene oxide ternary nanocomposites can be a promising candidate for supercapacitor applications (can be applied as a supercapacitor candidate). These results demonstrate that the ternary nanocomposite of mesoporous In_2O_3 cubes with π-electron-rich conductive nanocarbons of carbon nanotubes and reduced graphene oxide fabricated using a simple hydrothermal method could be an effective material for energy storage in high-performance supercapacitor applications.

Imae and co-workers fabricated conducting nanocomposites containing conductive polymer (polypyrrole or polyaniline), carbon nanohorn, and carbon dot through in-situ polymerization as electrode materials for supercapacitors [123]. A key factor is the presence of carbon dots. The addition of carbon dots to the nanocomposite systems efficiently increased the specific capacitance of the composite supercapacitors. In addition, the presence of carbon dots in the nanocomposite significantly enhanced capacitance retention. Thus, the nanoarchitected carbon composites would be promising materials for electrodes for energy storage devices in which high capacitance and stability can be expected. Imae and co-workers also fabricated nitrogen-doped graphene electrodes hybridized with magnetic metal oxide (NiO, Co_3O_4, or Fe_3O_4) as supercapacitors to an external magnetic field using a Helmholtz coil [124]. Electrical conductivity of the added metal oxides and the Lorentz force effect of the magnetic field showed some effects on the capacitance, the charge/discharge profile, and cycle retention. In particular, hybrid materials with Fe_3O_4 and nitrogen-doped graphene exhibited higher potential as supercapacitor electrodes with enhanced capacitance by the magnetic field.

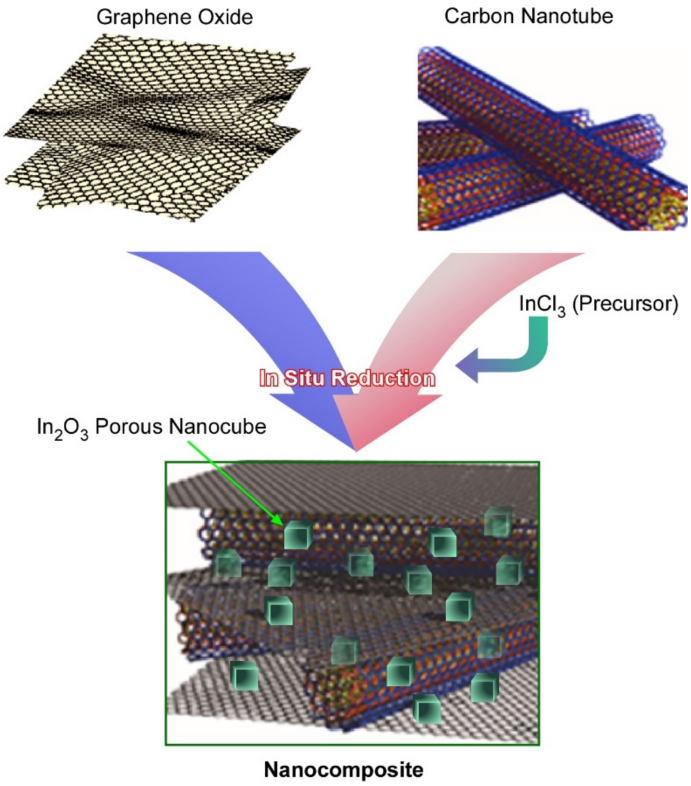

Figure 10. Fabrication of ternary nanocomposite material composed of mesoporous Indium oxide (In_2O_3) nanocubes embedded into carbon nanotubes and reduced graphene oxide.

6. Future Perspectives

This review briefly exhibited recent examples of carbon-related nanoarchitectonics for several functions. Although the described examples do not fully cover all the aspects, the selected examples demonstrated a wide range of synthetic possibilities, such as source applicability and fabrication methodologies. Functional carbon materials can be nanoarchitected through various processes, including (i) well-skilled organic synthesis with designed molecular sources, (ii) self-assembly of fullerenes under various conditions, (iii) practical low-cost synthesis from biomass, and (iv) hybrid/composite formation with various carbon sources. These examples strikingly demonstrated the enormous potentials of nanoarchitectonics approaches to produce functional carbon materials from various components such as small molecules, fullerene, other nanocarbons, and naturally abundant biomasses. Not limited to the energy-related usages such as supercapacitors described in this review, applications of the functional carbon materials for more advanced cells and batteries, environmental monitoring and remediation, biomedical usages, and advanced devices are also expected [125,126]. Furthermore, mechanisms for molecules and molecular assemblies coupled with carbon materials have to be further investigated [127–129]. Hybrids of polymers and nanocarbon materials with their percolative behaviors and their electrical/thermal properties have been investigated [130,131]. Nanoscale behaviors of these materials in terms of morphology, polymer nature, gained thermal properties (Joule effect), and electrical properties (increased electrical conductivity, piezoresistivity) were also discussed [132]. Electrocatalysis as an important branch of energy fields has been considered with carbon materials [133,134], which should be powerful outputs in applications of carbon nanoarchitectonics. Because biomass usages for carbon materials have much wider selections [135,136], carbon nanoarchitectonics with biomass have huge impacts in industrial applications.

Here, one particular target, carbon, was exemplified for nanoarchitectonics approaches to produce functional materials. However, the same methodology and similar processes would apply to a wide range of elements, molecular families, and related nanomateri-

als. Thus, further developments and expansion of the nanoarchitectonics concept would create a versatile paradigm to produce functional materials systems from any nanoscale components. Furthermore, emerging methods such as machine learning [137,138] would probably support efficient usages and developments of nanoarchitectonics strategies in materials science. Including various possibilities in carbon nanoarchitectonics, creating new functional materials with a combination of nanoarchitectonics and artificial intelligence will become a significant future challenge.

Author Contributions: All the authors contributed equally and jointly wrote this review article. All authors have read and agreed to the published version of the manuscript.

Funding: This work was partially supported by JSPS KAKENHI grant number JP20H00392, JP20H00316, JP20K05590, and JP21H04685.

Conflicts of Interest: The authors declare no conflict of interest.

References

1. Guo, D.; Shibuya, R.; Akiba, C.; Saji, S.; Kondo, T.; Nakamura, J. Active sites of nitrogen-doped carbon materials for oxygen reduction reaction clarified using model catalysts. *Science* **2016**, *351*, 361–365. [CrossRef] [PubMed]
2. Ohno, H.; Yoshizawa-Fujita, M.; Kohno, Y. Functional design of ionic liquids: Unprecedented liquids that contribute to energy technology, bioscience, and materials sciences. *Bull. Chem. Soc. Jpn.* **2019**, *92*, 852–868. [CrossRef]
3. Yamada, Y. Concentrated battery electrolytes: Developing new functions by manipulating the coordination states. *Bull. Chem. Soc. Jpn.* **2020**, *93*, 109–118. [CrossRef]
4. Wang, Q.; Domen, K. Particulate photocatalysts for light-driven water splitting: Mechanisms, challenges, and design strategies. *Chem. Rev.* **2020**, *120*, 919–985. [CrossRef] [PubMed]
5. Wang, C.; Cheng, P.; Yao, Y.; Yamauchi, Y.; Yan, X.; Li, J.; Na, J. In-situ fabrication of nanoarchitectured MOF filter for water purification. *J. Hazard. Mater.* **2020**, *392*, 122164. [CrossRef] [PubMed]
6. Pang, P.; Lai, Y.; Zhang, Y.; Wang, H.; Conlan, X.A.; Barrow, C.J.; Yang, W. Recent advancement of biosensor technology for the detection of microcystin-LR. *Bull. Chem. Soc. Jpn.* **2020**, *93*, 637–646. [CrossRef]
7. Yuan, G.; Li, F.; Li, K.; Liu, J.; Li, J.; Zhang, S.; Jia, Q.; Zhang, H. Research progress on photocatalytic reduction of Cr(VI) in polluted water. *Bull. Chem. Soc. Jpn.* **2021**, *94*, 1142–1155. [CrossRef]
8. Bhagat, J.; Nishimura, N.; Shimada, Y. Toxicological interactions of microplastics/nanoplastics and environmental contaminants: Current knowledge and future perspectives. *J. Hazard. Mater.* **2021**, *405*, 123913. [CrossRef]
9. Cabral, H.; Miyata, K.; Osada, K.; Kataoka, K. Block copolymer micelles in nanomedicine applications. *Chem. Rev.* **2018**, *118*, 6844–6892. [CrossRef]
10. Parthiban, V.; Yen, P.Y.M.; Uruma, Y.; Lai, P.-S. Designing synthetic glycosylated photosensitizers for photodynamic Therapy. *Bull. Chem. Soc. Jpn.* **2020**, *93*, 978–984. [CrossRef]
11. Komiyama, M. Molecular-level anatomy of SARS-CoV-2 for the battle against the COVID-19 pandemic. *Bull. Chem. Soc. Jpn.* **2021**, *94*, 1478–1490. [CrossRef]
12. Kim, K.; Bou-Ghannam, S.; Kameishi, S.; Oka, M.; Grainger, D.W.; Okano, T. Allogeneic mesenchymal stem cell sheet therapy: A new frontier in drug delivery systems. *J. Control. Release* **2021**, *330*, 696–704. [CrossRef] [PubMed]
13. Povie, G.; Segawa, Y.; Nishihara, T.; Miyauchi, Y.; Itami, K. Synthesis of a carbon nanobelt. *Science* **2017**, *356*, 172–175. [CrossRef] [PubMed]
14. Muramatsu, W.; Hattori, T.; Yamamoto, H. Game change from reagent- to substrate-controlled peptide synthesis. *Bull. Chem. Soc. Jpn.* **2020**, *93*, 759–767. [CrossRef]
15. Yamada, H.; Kuzuhara, D.; Suzuki, M.; Hayashi, H.; Aratani, N. Synthesis and morphological control of organic Semiconducting materials using the precursor approach. *Bull. Chem. Soc. Jpn.* **2020**, *93*, 1234–1267. [CrossRef]
16. Nothling, M.D.; Fu, Q.; Reyhani, A.; Allison-Logan, S.; Jung, K.; Zhu, J.; Kamigaito, M.; Boyer, C.; Qiao, G.G. Progress and perspectives beyond traditional RAFT polymerization. *Adv. Sci.* **2020**, *7*, 2001656. [CrossRef] [PubMed]
17. Yamago, S. Photoactivation of organotellurium compounds in precision polymer synthesis: Controlled radical polymerization and radical coupling reactions. *Bull. Chem. Soc. Jpn.* **2020**, *93*, 287–298. [CrossRef]
18. Teshima, Y.; Saito, M.; Mikie, T.; Komeyama, K.; Yoshida, H.; Osaka, I. Dithiazolylthienothiophene bisimide-based π-conjugated polymers: Improved synthesis and application to organic photovoltaics as P-type semiconductor. *Bull. Chem. Soc. Jpn.* **2020**, *93*, 561–567. [CrossRef]
19. Ariga, K.; Nishikawa, M.; Mori, T.; Takeya, J.; Shrestha, L.K.; Hill, J.P. Self-assembly as a key player for materials nanoarchitectonics. *Sci. Technol. Adv. Mater.* **2019**, *20*, 51–95. [CrossRef] [PubMed]
20. Datta, S.; Kato, Y.; Higashiharaguchi, S.; Aratsu, K.; Isobe, A.; Saito, T.; Prabhu, D.D.; Kitamoto, Y.; Hollamby, M.J.; Smith, A.J.; et al. Self-assembled poly-catenanes from supramolecular toroidal building blocks. *Nature* **2010**, *583*, 400–405. [CrossRef] [PubMed]

21. Kato, T.; Gupta, M.; Yamaguchi, D.; Gan, K.P.; Nakayama, M. Supramolecular association and nanostructure formation of liquid crystals and polymers for new functional materials. *Bull. Chem. Soc. Jpn.* **2021**, *94*, 357–376. [CrossRef]
22. Percec, V.; Xiao, Q. Helical self-organizations and emerging functions in architectures, biological and synthetic macromolecules. *Bull. Chem. Soc. Jpn.* **2021**, *94*, 900–928. [CrossRef]
23. Zheng, S.; Li, Q.; Xue, H.; Pang, H.; Xu, Q. A highly alkaline-stable metal oxide@metal–organic framework composite for high-performance electrochemical energy storage. *Natl. Sci. Rev.* **2020**, *7*, 305–314. [CrossRef]
24. Paris, J.L.; Vallet-Regí, M. Ultrasound-activated nanomaterials for therapeutics. *Bull. Chem. Soc. Jpn.* **2020**, *93*, 220–229. [CrossRef]
25. Yang, G.; Kuwahara, Y.; Mori, K.; Louis, C.; Yamashita, H. PdAg alloy nanoparticles encapsulated in N-doped microporous hollow carbon spheres for hydrogenation of CO_2 to formate. *Appl. Catal. B Environ.* **2021**, *283*, 119628. [CrossRef]
26. Yamashita, M. Next generation multifunctional nano-science of advanced metal complexes with quantum effect and nonlinearity. *Bull. Chem. Soc. Jpn.* **2021**, *94*, 209–264. [CrossRef]
27. Kimura, K.; Miwa, K.; Imada, H.; Imai-Imada, M.; Kawahara, S.; Takeya, J.; Kawai, M.; Galperin, M.; Kim, Y. Selective triplet exciton formation in a single molecule. *Nature* **2019**, *570*, 210–213. [CrossRef]
28. Hasegawa, T.; Shioya, N. MAIRS: Innovation of molecular orientation analysis in a thin film. *Bull. Chem. Soc. Jpn.* **2020**, *93*, 1127–1138. [CrossRef]
29. Kazuma, E. Real-space studies of plasmon-induced dissociation reactions with an STM. *Bull. Chem. Soc. Jpn.* **2020**, *93*, 1552–1557. [CrossRef]
30. Nakaya, M.; Tsukamoto, S.; Kuwahara, Y.; Aono, M.; Nakayama, T. Molecular scale control of unbound and bound C_{60} for topochemical ultradense data storage in an ultrathin C_{60} film. *Adv. Mater.* **2010**, *22*, 1622–1625. [CrossRef]
31. Rao, C.N.R.; Pramoda, K. Borocarbonitrides, BxCyNz, 2D nanocomposites with novel properties. *Bull. Chem. Soc. Jpn.* **2019**, *92*, 441–468. [CrossRef]
32. Ono, M.; Hata, M.; Tsunekawa, M.; Nozaki, K.; Sumikura, H.; Chiba, H.; Notomi, M. Ultrafast and energy-efficient all-optical switching with graphene-loaded deep-subwavelength plasmonic waveguides. *Nat. Photonics* **2020**, *14*, 37–43. [CrossRef]
33. Shimizu, T.; Lungerich, D.; Stuckner, J.; Murayama, M.; Harano, K.; Nakamura, E. Real-time video imaging of mechanical motions of a single molecular shuttle with sub-millisecond sub-angstrom precision. *Bull. Chem. Soc. Jpn.* **2020**, *93*, 1079–1085. [CrossRef]
34. Kamei, K.; Shimizu, T.; Harano, K.; Nakamura, E. Aryl radical addition to curvatures of carbon nanohorns for single-molecule-level molecular imaging. *Bull. Chem. Soc. Jpn.* **2020**, *93*, 1603–1608. [CrossRef]
35. Ariga, K.; Ji, Q.; Nakanishi, W.; Hill, J.P.; Aono, M. Nanoarchitectonics: A new materials horizon for nanotechnology. *Mater. Horiz.* **2015**, *2*, 406–413. [CrossRef]
36. Ariga, K. Nanoarchitectonics revolution and evolution: From small science to big technology. *Small Sci.* **2021**, *1*, 2000032. [CrossRef]
37. Ariga, K.; Ji, Q.; Hill, J.; Bando, Y.; Aono, M. Forming nanomaterials as layered functional structures toward materials nanoarchitectonics. *NPG Asia Mater.* **2012**, *4*, e17. [CrossRef]
38. Ariga, K. Nanoarchitectonics: What's coming next after nanotechnology? *Nanoscale Horiz.* **2021**, *6*, 364–378. [CrossRef]
39. Aono, M.; Ariga, K. The way to nanoarchitectonics and the way of nanoarchitectonics. *Adv. Mater.* **2016**, *28*, 989–992. [CrossRef]
40. Ariga, K.; Minami, K.; Ebara, M.; Nakanishu, J. What are the emerging concepts and challenges in NANO? Nanoarchitectonics, hand-operating nanotechnology and mechanobiology. *Polym. J.* **2016**, *48*, 371–389. [CrossRef]
41. Ariga, K.; Li, J.; Fei, J.; Ji, Q.; Hill, J.P. Nanoarchitectonics for dynamic functional materials from atomic-/molecular-level manipulation to macroscopic action. *Adv. Mater.* **2016**, *28*, 1251–1286. [CrossRef]
42. Ariga, K.; Jia, X.; Song, J.; Hill, J.P.; Leong, D.T.; Jia, Y.; Li, J. Nanoarchitectonics beyond self-assembly: Challenges to create bio-like hierarchic organization. *Angew. Chem. Int. Ed.* **2020**, *59*, 15424–15446. [CrossRef]
43. Komiyama, M.; Mori, T.; Ariga, K. Molecular imprinting: Materials nanoarchitectonics with molecular information. *Bull. Chem. Soc. Jpn.* **2018**, *91*, 1075–1111. [CrossRef]
44. Tirayaphanitchkul, C.; Imwiset, K.; Ogawa, M. Nanoarchitectonics through organic modification of oxide based layered materials; concepts, methods and functions. *Bull. Chem. Soc. Jpn.* **2021**, *94*, 678–693. [CrossRef]
45. Ariga, K.; Mori, T.; Kitao, T.; Uemura, T. Supramolecular chiral nanoarchitectonics. *Adv. Mater.* **2020**, *32*, 1905657. [CrossRef]
46. Eguchi, M.; Nugraha, A.S.; Rowan, A.E.; Shapter, J.; Yamauchi, Y. Adsorchromism: Molecular nanoarchitectonics at 2D nanosheets—Old chemistry for advanced chromism. *Adv. Sci.* **2021**, *8*, 2100539. [CrossRef] [PubMed]
47. Ariga, K.; Shionoya, M. Nanoarchitectonics for coordination asymmetry and related chemistry. *Bull. Chem. Soc. Jpn.* **2021**, *94*, 839–859. [CrossRef]
48. Ishihara, S.; Labuta, J.; Van Rossom, W.; Ishikawa, D.; Minami, K.; Hill, J.P.; Ariga, K. Porphyrin-based sensor nanoarchitectonics in diverse physical detection modes. *Phys. Chem. Chem. Phys.* **2014**, *16*, 9713–9746. [CrossRef] [PubMed]
49. Liu, J.; Zhou, H.; Yang, W.; Ariga, K. Soft nanoarchitectonics for enantioselective biosensing. *Acc. Chem. Res.* **2020**, *53*, 644–653. [CrossRef]
50. Giussi, J.M.; Cortez, M.L.; Marmisollé, W.A.; Azzaroni, O. Practical use of polymer brushes in sustainable energy applications: Interfacial nanoarchitectonics for high-efficiency devices. *Chem. Soc. Rev.* **2019**, *48*, 814–849. [CrossRef]
51. Ariga, K.; Ito, M.; Mori, T.; Watanabe, S.; Takeya, J. Atom/molecular nanoarchitectonics for devices and related applications. *Nano Today* **2019**, *28*, 100762. [CrossRef]

52. Wu, F.; Eid, K.; Abdullah, A.M.; Niu, W.; Wang, C.; Lan, Y.; Elzatahry, A.A.; Xu, G. Unveiling one-pot template-free fabrication of exquisite multidimensional PtNi multicube nanoarchitectonics for the efficient electrochemical oxidation of ethanol and methanol with a great tolerance for CO. *ACS Appl. Mater. Interfaces* **2020**, *12*, 31309–31318. [CrossRef]
53. Kumari, N.; Kumar, A.; Krishnan, V. Ultrathin Au–Ag heterojunctions on nanoarchitectonics based biomimetic substrates for dip catalysis. *J. Inorg. Organomet. Polym.* **2021**, *31*, 1954–1966. [CrossRef]
54. Kim, J.; Kim, J.H.; Ariga, K. Redox-active polymers for energy storage nanoarchitectonics. *Joule* **2017**, *1*, 739–768. [CrossRef]
55. Azhar, A.; Li, Y.; Cai, Z.; Zakaria, M.B.; Masud, M.K.; Hossain, M.S.A.; Kim, J.; Zhang, W.; Na, J.; Yamauchi, Y.; et al. Nanoarchitectonics: A new materials horizon for Prussian blue and its analogues. *Bull. Chem. Soc. Jpn.* **2019**, *92*, 875–904. [CrossRef]
56. Pham, T.-A.; Qamar, A.; Dinh, T.; Masud, M.K.; Rais-Zadeh, M.; Senesky, D.G.; Yamauchi, Y.; Nguyen, N.-T.; Phan, H.-P. Nanoarchitectonics for wide bandgap semiconductor nanowires: Toward the Next generation of nanoelectromechanical systems for environmental monitoring. *Adv. Sci.* **2020**, *7*, 2001294. [CrossRef] [PubMed]
57. Sciortino, F.; Sanchez-Ballester, N.M.; Mir, S.H.; Rydzek, G. Functional elastomeric copolymer membranes designed by nanoarchitectonics approach for methylene blue removal. *J. Inorg. Organomet. Polym.* **2021**, *31*, 1967–1977. [CrossRef]
58. Rozhina, E.; Ishmukhametov, I.; Batasheva, S.; Akhatova, F.; Fakhrullin, R. Nanoarchitectonics meets cell surface engineering: Shape recognition of human cells by halloysite-doped silica cell imprints. *Beilstein J. Nanotechnol.* **2019**, *10*, 1818–1825. [CrossRef]
59. Zhao, L.; Zou, Q.; Yan, X. Self-assembling peptide-based nanoarchitectonics. *Bull. Chem. Soc. Jpn.* **2019**, *92*, 70–79. [CrossRef]
60. Liang, X.; Li, L.; Tang, J.; Komiyama, K.; Ariga, K. Dynamism of supramolecular DNA/RNA nanoarchitectonics: From interlocked structures to molecular machines. *Bull. Chem. Soc. Jpn.* **2020**, *93*, 581–603. [CrossRef]
61. Karthick, V.; Kumar, D.; Ariga, K.; Kumar, C.M.V.; Kumar, V.G.; Vasanth, K.; Dhas, T.S.; Ravi, M.; Baalamurugan, J. Incorporation of 5-nitroisatin for tailored hydroxyapatite nanorods and its effect on cervical cancer cells: A nanoarchitectonics approach. *J. Inorg. Organomet. Polym.* **2021**, *31*, 1946–1953. [CrossRef]
62. Nandgude, T.; Kawtikwar, A. Nanoarchitectonics: A new horizon for drug targeting. *J. Pharm. Innov.* **2021**, in press. [CrossRef]
63. Karthik, V.; Poornima, S.; Vigneshwaran, A.; Raj, D.P.R.D.D.; Subbaiya, R.; Manikandan, S.; Saravanan, M. Nanoarchitectonics is an emerging drug/gene delivery and targeting strategy—A critical review. *J. Mol. Struct.* **2021**, *1243*, 130844. [CrossRef]
64. Ariga, K.; Shrestha, L.K. Zero-to-one (or more) nanoarchitectonics: How to produce functional materials from zero-dimensional single-element unit, fullerene. *Mater. Adv.* **2021**, *2*, 582–597. [CrossRef]
65. Maji, S.; Shrestha, L.K.; Ariga, K. Nanoarchitectonics for hierarchical fullerene nanomaterials. *Nanomaterials* **2021**, *11*, 2146. [CrossRef]
66. Kanao, E.; Kubo, T.; Otsuka, K. Carbon-based nanomaterials for separation media. *Bull. Chem. Soc. Jpn.* **2020**, *93*, 482–489. [CrossRef]
67. Zhu, H.; Hong, L.; Tanaka, H.; Ma, X.; Yang, C. Facile solvent mixing strategy for extracting highly enriched (6,5)single-walled carbon nanotubes in improved yield. *Bull. Chem. Soc. Jpn.* **2021**, *94*, 1166–1171. [CrossRef]
68. Alabadi, A.A.; Abbood, H.A.; Dawood, A.S.; Tan, B. Ultrahigh-CO_2 adsorption capacity and CO_2/N_2 selectivity by nitrogen-doped porous activated carbon monolith. *Bull. Chem. Soc. Jpn.* **2020**, *93*, 421–426. [CrossRef]
69. Miyashiro, D.; Hamano, R.; Umemura, K. A review of applications using mixed materials of cellulose, nanocellulose and carbon nanotubes. *Nanomaterials* **2020**, *10*, 186. [CrossRef]
70. Permatasari, F.A.; Irham, M.A.; Bisri, S.Z.; Iskandar, F. Carbon-based quantum dots for supercapacitors: Recent advances and future challenges. *Nanomaterials* **2021**, *11*, 91. [CrossRef]
71. Saito, Y.; Ashizawa, M.; Matsumoto, H. Mesoporous hydrated graphene nanoribbon electrodes for efficient supercapacitors: Effect of nanoribbon dispersion on pore structure. *Bull. Chem. Soc. Jpn.* **2020**, *93*, 1268–1274. [CrossRef]
72. Kawaura, H.; Harada, M.; Kondo, Y.; Mizutani, M.; Takahashi, N.; Yamada, N.I. Operando time-slicing neutron reflectometry measurements of solid electrolyte interphase formation on amorphous carbon surfaces of a Li-ion battery. *Bull. Chem. Soc. Jpn.* **2020**, *93*, 854–861. [CrossRef]
73. Matsuo, Y. Creation of highly efficient and durable organic and perovskite solar cells using nanocarbon materials. *Bull. Chem. Soc. Jpn.* **2021**, *94*, 1080–1089. [CrossRef]
74. Xu, X.; Müllen, K.; Narita, A. Syntheses and characterizations of functional polycyclic aromatic hydrocarbons and graphene nanoribbons. *Bull. Chem. Soc. Jpn.* **2020**, *93*, 490–506. [CrossRef]
75. Xu, X.; Kinikar, A.; Giovannantonio, M.D.; Ruffieux, R.; Müllen, K.; Fasel, R.; Narita, A. On-surface synthesis of dibenzohexacenohexacene and dibenzopentaphenoheptaphene. *Bull. Chem. Soc. Jpn.* **2021**, *94*, 997–999. [CrossRef]
76. Kato, K.; Takaba, K.; Maki-Yonekura, S.; Mitoma, N.; Nakanishi, Y.; Nishihara, T.; Hatakeyama, T.; Kawada, T.; Hijikata, Y.; Pirillo, J.; et al. Double-helix supramolecular nanofibers assembled from negatively curved nanographenes. *J. Am. Chem. Soc.* **2021**, *143*, 5465–5469. [CrossRef] [PubMed]
77. Sun, Z.; Ikemoto, K.; Fukunaga, T.M.; Koretsune, T.; Arita, R.; Sato, S.; Isobe, H. Finite phenine nanotubes with periodic vacancy defects. *Science* **2019**, *363*, 151–155. [CrossRef]
78. Mori, T.; Tanaka, H.; Dalui, A.; Mitoma, N.; Suzuki, K.; Matsumoto, M.; Aggarwal, N.; Patnaik, A.; Acharya, S.; Shrestha, L.K.; et al. Carbon nanosheets by morphology-retained carbonization of two-dimensional assembled anisotropic carbon nanorings. *Angew. Chem. Int. Ed.* **2018**, *57*, 9679–9683. [CrossRef]

79. Krishnan, V.; Kasuya, Y.; Ji, Q.; Sathish, M.; Shrestha, L.K.; Ishihara, S.; Minami, K.; Morita, H.; Yamazaki, Y.; Hanagata, N.; et al. Vortex-aligned fullerene nanowhiskers as a scaffold for orienting cell growth. *ACS Appl. Mater. Interfaces* **2015**, *7*, 15667–15673. [CrossRef] [PubMed]
80. Ariga, K.; Mori, T.; Li, J. Langmuir nanoarchitectonics from basic to frontier. *Langmuir* **2019**, *35*, 3585–3599. [CrossRef] [PubMed]
81. Ariga, K. Don't forget Langmuir–Blodgett films 2020: Interfacial nanoarchitectonics with molecules, materials, and living objects. *Langmuir* **2020**, *36*, 7158–7180. [CrossRef]
82. Matsumoto, I.; Sekiya, R.; Haino, T. Nanographenes from distinct carbon sources. *Bull. Chem. Soc. Jpn.* **2021**, *94*, 1394–1399. [CrossRef]
83. Yamaguchi, A.; Edanami, Y.; Yamaguchi, T.; Shibuya, Y.; Fukaya, N.; Kohzuma, T. Effect of cavity size of mesoporous silica on type 1 copper site geometry in Pseudoazurin. *Bull. Chem. Soc. Jpn.* **2020**, *93*, 630–636. [CrossRef]
84. Kankala, R.K.; Han, Y.-H.; Na, J.; Lee, C.-H.; Sun, Z.; Wang, S.-B.; Kimura, T.; Ok, Y.S.; Yamauchi, Y.; Chen, A.-Z.; et al. Nanoarchitectured structure and surface biofunctionality of mesoporous silica nanoparticles. *Adv. Mater.* **2020**, *32*, 1907035. [CrossRef] [PubMed]
85. Singh, B.; Na, J.; Konarova, M.; Wakihara, T.; Yamauchi, Y.; Salomon, C.; Gawande, M.B. Functional mesoporous silica nanomaterials for catalysis and environmental applications. *Bull. Chem. Soc. Jpn.* **2020**, *93*, 1459–1496. [CrossRef]
86. Guo, J.; Huo, J.; Liu, Y.; Wu, W.; Wang, Y.; Wu, M.; Liu, H.; Wang, G. Nitrogen-doped porous carbon supported nonprecious metal single-atom electrocatalysts: From Synthesis to application. *Small Methods* **2019**, *3*, 1900159. [CrossRef]
87. Joseph, S.; Saianand, G.; Benzigar, M.R.; Ramadass, K.; Singh, G.; Gopalan, A.-I.; Yang, J.H.; Mori, T.; Al-Muhtaseb, A.H.; Yi, J.; et al. Recent advances in functionalized nanoporous carbons derived from waste resources and their applications in energy and environment. *Adv. Sustain. Syst.* **2021**, *5*, 2000169. [CrossRef]
88. Singh, G.; Lee, J.M.; Kothandam, G.; Palanisami, T.; Al-Muhtaseb, A.H.; Karakoti, A.; Yi, J.; Bolan, N.; Vinu, A. A review on the synthesis and applications of nanoporous carbons for the removal of complex chemical contaminants. *Bull. Chem. Soc. Jpn.* **2021**, *94*, 1232–1257. [CrossRef]
89. Shitanda, I.; Kato, T.; Suzuki, R.; Aikawa, T.; Hoshi, Y.; Itagaki, M.; Tsujimura, S. Mesoporous carbon by graft polymerization of poly(glycidyl methacrylate). *Bull. Chem. Soc. Jpn.* **2020**, *93*, 32–36. [CrossRef]
90. Baskar, A.V.; Ruban, A.M.; Davidraj, J.M.; Singh, G.; Al-Muhtaseb, A.H.; Lee, J.M.; Yi, J.; Vinu, A. Single-step synthesis of 2D mesoporous C_{60}/carbon hybrids for supercapacitor and Li-ion battery applications. *Bull. Chem. Soc. Jpn.* **2021**, *94*, 133–140. [CrossRef]
91. Zhao, Y.; Shao, L.; Li, L.; Wang, S.; Song, G.; Gao, Z.; Zhang, X.; Wang, T.; Li, Y.; Zhang, L.; et al. Novel zinc-based infinite coordination polymer for highly selective ammonia gas sensing at room temperature. *Bull. Chem. Soc. Jpn.* **2020**, *93*, 1070–1073. [CrossRef]
92. Xiao, X.; Zou, L.; Pang, H.; Xu, Q. Synthesis of micro/nanoscaled metal–organic frameworks and their direct electrochemical applications. *Chem. Soc. Rev.* **2020**, *49*, 301–331. [CrossRef] [PubMed]
93. Hosono, N. Design of porous coordination materials with dynamic properties. *Bull. Chem. Soc. Jpn.* **2021**, *94*, 60–69. [CrossRef]
94. Li, Y.; Henzie, J.; Park, T.; Wang, J.; Young, C.; Xie, H.; Yi, J.W.; Li, J.; Kim, M.; Kim, J.; et al. Fabrication of flexible microsupercapacitors with binder-free ZIF-8 derived carbon films via electrophoretic deposition. *Bull. Chem. Soc. Jpn.* **2020**, *93*, 176–181. [CrossRef]
95. Geng, K.; He, T.; Liu, R.; Dalapati, S.; Tan, K.T.; Li, Z.; Tao, S.; Gong, Y.; Jiang, Q.; Jiang, D. Covalent organic frameworks: Design, synthesis, and functions. *Chem. Rev.* **2020**, *120*, 8814–8933. [CrossRef]
96. Bai, B.; Wang, D.; Wan, L.-J. Synthesis of covalent organic framework films at interfaces. *Bull. Chem. Soc. Jpn.* **2021**, *94*, 1090–1098. [CrossRef]
97. Jiang, D. Covalent organic frameworks: A molecular platform for designer polymeric architectures and functional materials. *Bull. Chem. Soc. Jpn.* **2021**, *94*, 1215–1231. [CrossRef]
98. Kim, G.; Shiraki, T.; Fujigaya, T. Thermal conversion of triazine-based covalent organic frameworks to nitrogen-doped nanoporous carbons and their capacitor performance. *Bull. Chem. Soc. Jpn.* **2020**, *93*, 414–420. [CrossRef]
99. Neal, E.A.; Nakanishi, T. Alkyl-fullerene materials of tunable morphology and function. *Bull. Chem. Soc. Jpn.* **2021**, *94*, 1769–1788. [CrossRef]
100. Chen, G.; Shrestha, L.K.; Ariga, K. Zero-to-two nanoarchitectonics: Fabrication of two-dimensional materials from zero-dimensional fullerene. *Molecules* **2021**, *26*, 4636. [CrossRef] [PubMed]
101. Akiyama, T. Development of fullerene thin-film assemblies and fullerene-diamine adducts towards practical nanocarbon-based electronic materials. *Bull. Chem. Soc. Jpn.* **2019**, *92*, 1181–1199. [CrossRef]
102. Minami, K.; Song, J.; Shrestha, L.K.; Ariga, K. Nanoarchitectonics for fullerene biology. *Appl. Mater. Today* **2021**, *23*, 100989. [CrossRef]
103. Bairi, P.; Maji, S.; Hill, J.P.; Kim, J.H.; Ariga, K.; Shrestha, L.K. Mesoporous carbon cubes derived from fullerene crystals as a high rate performance electrode material for supercapacitors. *J. Mater. Chem. A* **2019**, *7*, 12654–12660. [CrossRef]
104. Maji, S.; Shrestha, R.G.; Lee, J.; Han, S.A.; Hill, J.P.; Kim, J.H.; Ariga, K.; Shrestha, L.K. Macaroni fullerene crystals-derived mesoporous carbon tubes as a high rate performance supercapacitor electrode material. *Bull. Chem. Soc. Jpn.* **2021**, *94*, 1502–1509. [CrossRef]

105. Shrestha, L.K.; Shrestha, R.G.; Yamauchi, Y.; Hill, J.P.; Nishimura, T.; Miyazawa, K.; Kawai, T.; Okada, S.; Wakabayashi, K.; Ariga, K. Nanoporous carbon tubes from fullerene crystals as the π-electron carbon source. *Angew. Chem. Int. Ed.* **2015**, *54*, 951–955. [CrossRef] [PubMed]
106. Bairi, P.; Shrestha, R.G.; Hill, J.P.; Nishimura, T.; Ariga, K.; Shrestha, L.K. Mesoporous graphitic carbon microtubes derived from fullerene C_{70} tubes as a high performance electrode material for advanced supercapacitors. *J. Mater. Chem. A* **2016**, *4*, 13899–13906. [CrossRef]
107. Gao, T.; Xu, C.; Li, R.; Zhang, R.; Wang, B.; Jiang, X.; Hu, M.; Bando, Y.; Kong, D.; Dai, P.; et al. Biomass-derived carbon paper to sandwich magnetite anode for long-life Li-ion battery. *ACS Nano* **2019**, *13*, 11901–11911. [CrossRef] [PubMed]
108. Lu, T.; Liu, Y.; Xu, X.; Pan, L.; Alothman, A.A.; Shapter, J.; Wang, Y.; Yamauchi, Y. Highly efficient water desalination by capacitive deionization on biomass-derived porous carbon nanoflakes. *Sep. Purif. Technol.* **2021**, *256*, 117771. [CrossRef]
109. Shrestha, L.K.; Adhikari, L.; Shrestha, R.G.; Adhikari, M.P.; Adhikari, R.; Hill, J.P.; Pradhananga, R.R.; Ariga, K. Nanoporous carbon materials with enhanced supercapacitance performance and non-aromatic chemical sensing with C_1/C_2 alcohol discrimination. *Sci. Technol. Adv. Mater.* **2016**, *17*, 483–492. [CrossRef]
110. Furuuchi, N.; Shrestha, R.G.; Yamashita, Y.; Hirao, T.; Ariga, K.; Shrestha, L.K. Self-assembled fullerene crystals as excellent aromatic vapor sensors. *Sensors* **2019**, *19*, 267. [CrossRef]
111. Torad, N.L.; Ding, B.; El-Said, W.A.; El-Hady, D.A.; Alshitari, W.; Na, J.; Yamauchi, Y.; Zhang, X. MOF-derived hybrid nanoarchitectured carbons for gas discrimination of volatile aromatic hydrocarbons. *Carbon* **2020**, *168*, 55–64. [CrossRef]
112. Lu, T.; Xu, X.; Zhang, S.; Pan, L.; Wang, Y.; Alshehri, S.M.; Ahamad, T.; Kim, M.; Na, J.; Hossain, M.S.A.; et al. High-performance capacitive deionization by lignocellulose-derived eco-friendly porous carbon materials. *Bull. Chem. Soc. Jpn.* **2020**, *93*, 1014–1019. [CrossRef]
113. Sheng, X.; Xu, X.; Wu, Y.; Zhang, X.; Lin, P.; Eid, K.; Abdullah, A.M.; Li, Z.; Yang, T.; Nanjundan, A.K.; et al. Nitrogenization of biomass-derived porous carbon microtubes promotes capacitive deionization performance. *Bull. Chem. Soc. Jpn.* **2021**, *94*, 1645–1650. [CrossRef]
114. Liu, H.; Chen, W.; Zhang, R.; Ren, Y. Naturally O-N-S co-doped carbon with multiscale pore architecture derived from lotus leaf stem for high-performance supercapacitors. *Bull. Chem. Soc. Jpn.* **2021**, *94*, 1705–1714. [CrossRef]
115. Shrestha, L.K.; Shrestha, R.G.; Maji, S.; Pokharel, B.P.; Rajbhandari, R.; Shrestha, R.L.; Pradhananga, R.R.; Hill, J.P.; Ariga, K. High surface area nanoporous graphitic carbon materials derived from Lapsi seed with enhanced supercapacitance. *Nanomaterials* **2020**, *10*, 728. [CrossRef]
116. Shrestha, R.L.; Shrestha, T.; Tamrakar, B.M.; Shrestha, R.G.; Maji, S.; Ariga, K.; Shrestha, L.K. Nanoporous carbon materials derived from Washnut seed with enhanced supercapacitance. *Materials* **2020**, *13*, 2371. [CrossRef]
117. Kim, J.; Park, S.-J.; Chung, S.; Kim, S. Preparation and capacitance of Ni metal organic framework/reduced graphene oxide composites for supercapacitors as nanoarchitectonics. *J. Nanosci. Nanotechnol.* **2020**, *20*, 2750–2754. [CrossRef]
118. Boukhalfa, N.; Darder, M.; Boutahala, M.; Aranda, P.; Ruiz-Hitzky, E. Composite nanoarchitectonics: Alginate beads encapsulating sepiolite/magnetite/Prussian blue for removal of cesium ions from water. *Bull. Chem. Soc. Jpn.* **2021**, *94*, 122–132. [CrossRef]
119. Mool-am-kha, P.; Themsirimongkon, S.; Saipanya, S.; Saianand, G.; Tuantranont, A.; Karuwan, C.; Jakmunee, J. Hybrid electrocatalytic nanocomposites based on carbon nanotubes/nickel oxide/nafion toward an individual and simultaneous determination of serotonin and dopamine in human serum. *Bull. Chem. Soc. Jpn.* **2020**, *93*, 1393–1400. [CrossRef]
120. Wang, Q.; Wu, M.; Meng, S.; Zang, X.; Dai, Z.; Si, W.; Huang, W.; Dong, X. Hydrazine sensor based on Co_3O_4/rGO/carbon cloth electrochemical electrode. *Adv. Mater. Interfaces* **2016**, *3*, 1500691. [CrossRef]
121. Mondal, S.; Rana, U.; Malik, S. Reduced graphene oxide/Fe_3O_4/polyaniline nanostructures as electrode materials for an all-solid-state hybrid supercapacitor. *J. Phys. Chem. C* **2017**, *121*, 7573–7583. [CrossRef]
122. Sengottaiyan, C.; Jayavel, R.; Shrestha, R.G.; Subramani, T.; Maji, S.; Kim, J.H.; Hill, J.P.; Ariga, K.; Shrestha, L.K. Indium oxide/carbon nanotube/reduced graphene oxide ternary nanocomposite with enhanced electrochemical supercapacitance. *Bull. Chem. Soc. Jpn.* **2019**, *92*, 521–528. [CrossRef]
123. Chang, C.C.; Geleta, T.A.; Imae, T. Effect of carbon dots on supercapacitor performance of carbon nanohorn/conducting polymer composites. *Bull. Chem. Soc. Jpn.* **2021**, *94*, 454–462. [CrossRef]
124. Fite, M.C.; Rao, J.-Y.; Imae, T. Effect of external magnetic field on hybrid supercapacitors of nitrogen-doped graphene with magnetic metal oxides. *Bull. Chem. Soc. Jpn.* **2020**, *93*, 1139–1149. [CrossRef]
125. Inagaki, M.; Toyoda, M.; Soneda, Y.; Morishita, T. Nitrogen-doped carbon materials. *Carbon* **2018**, *132*, 104–140. [CrossRef]
126. Wang, C.; Kim, J.; Tang, J.; Kim, M.; Lim, H.; Malgras, V.; You, J.; Xu, Q.; Li, J.; Yamauchi, Y. New strategies for novel MOF-derived carbon materials based on nanoarchitectures. *Chem* **2020**, *6*, 19–40. [CrossRef]
127. Weerathunga, D.T.D.; Jayawickrama, S.M.; Phua, Y.K.; Nobori, K.; Fujigaya, T. Effect of polytetrafluoroethylene particles in cathode catalyst layer based on carbon nanotube for polymer electrolyte membrane fuel cells. *Bull. Chem. Soc. Jpn.* **2019**, *92*, 2038–2042. [CrossRef]
128. Stefanopoulos, K.L.; Tampaxis, C.; Sapalidis, A.A.; Katsaros, F.K.; Youngs, T.G.A.; Bowron, D.T.; Steriotis, T.A. Total neutron scattering study of supercooled CO_2 confined in an ordered mesoporous carbon. *Carbon* **2010**, *167*, 296–306. [CrossRef]
129. Harano, K. Self-assembly mechanism in nucleation processes of molecular cystalline materials. *Bull. Chem. Soc. Jpn.* **2021**, *94*, 463–472. [CrossRef]

130. Hezaveh, S.; Samanta, S.; Milano, G.; Roccatano, D. Molecular dynamics simulation study of solvent effects on conformation and dynamics of polyethylene oxide and polypropylene oxide chains in water and in common organic solvents. *J. Chem. Phys.* **2012**, *136*, 124901. [CrossRef]
131. Zhao, Y.; Byshkin, M.; Cong, Y.; Kawakatsu, T.; Guadagno, L.; Nicola, A.D.; Yu, N.; Milano, G.; Dong, B. Self-assembly of carbon nanotubes in polymer melts: Simulation of structural and electrical behaviour by hybrid particle-field molecular dynamics. *Nanoscale* **2016**, *8*, 15538–15552. [CrossRef]
132. Donati, G.; De Nicola, A.; Munaò, G.; Byshkin, M.; Vertuccio, L.; Guadagno, L.; Le Gofff, R.; Milanoa, G. Simulation of self-heating process on the nanoscale: A multiscale approach for molecular models of nanocomposite materials. *Nanoscale Adv.* **2020**, *2*, 3164–3180. [CrossRef]
133. Zhang, W.; Wu, Z.-Y.; Jiang, H.-L.; Yu, S.-H. Nanowire-directed templating synthesis of metal-organic framework nanofibers and their derived porous doped carbon nanofibers for enhanced electrocatalysis. *J. Am. Chem. Soc.* **2014**, *136*, 14385–14388. [CrossRef]
134. Wu, Z.-Y.; Xu, X.-X.; Hu, B.-C.; Liang, H.-W.; Lin, Y.; Chen, L.-F.; Yu, S.-H. Iron carbide nanoparticles encapsulated in mesoporous Fe-N-doped carbon nanofibers for efficient electrocatalysis. *Angew. Chem. Int. Ed.* **2015**, *54*, 8179–8183. [CrossRef]
135. Wu, Z.-Y.; Li, C.; Liang, H.-W.; Chen, J.-F.; Yu, S.-H. Ultralight, flexible, and fire-resistant carbon nanofiber aerogels. *Angew. Chem. Int. Ed.* **2013**, *52*, 2925–2929. [CrossRef] [PubMed]
136. Wu, Z.-Y.; Liang, H.-W.; Li, C.; Hu, B.-C.; Xu, X.-X.; Wang, Q.; Chen, J.-F.; Yu, S.-H. Dyeing bacterial cellulose pellicles for energetic heteroatom doped carbon nanofiber aerogels. *Nano Res.* **2014**, *7*, 1861–1872. [CrossRef]
137. Sumita, M.; Tamura, R.; Homma, K.; Kaneta, C.; Tsuda, K. Li-ion conductive Li_3PO_4-Li_3BO_3-Li_2SO_4 mixture: Prevision through density functional molecular dynamics and machine learning. *Bull. Chem. Soc. Jpn.* **2019**, *92*, 1100–1106. [CrossRef]
138. Toyao, T.; Maeno, Z.; Takakusagi, S.; Kamachi, T.; Takigawa, I.; Shimizu, K. Machine learning for catalysis informatics: Recent applications and prospects. *ACS Catal.* **2020**, *10*, 2260–2297. [CrossRef]